Electronic Supplementary Material (ESI) for Physical Chemistry Chemical Physics.

The interactions of chelate-based ionic liquids: from the perspective of vaporization enthalpy

Sijie Song[a], Songna Zhang[a], Jia Yao[*a] and Haoran Li[*a,b]

a *Miss. S. Song, Dr. S. Zhang, Prof. J. Yao, Prof. H. Li*
Department of Chemistry
ZJU-NHU United R&D Center
Zhejiang University, Hangzhou 310027 (China)
E-mail: yaojia@zju.edu.cn, lihr@zju.edu.cn
b *Prof. H. Li*
State Key Laboratory of Chemical Engineering
College of Chemical and Biological Engineering
Zhejiang University, Hangzhou, 310027 (China).

Synthesis steps

Scheme S1. Three-step approach for synthesis of ChILs

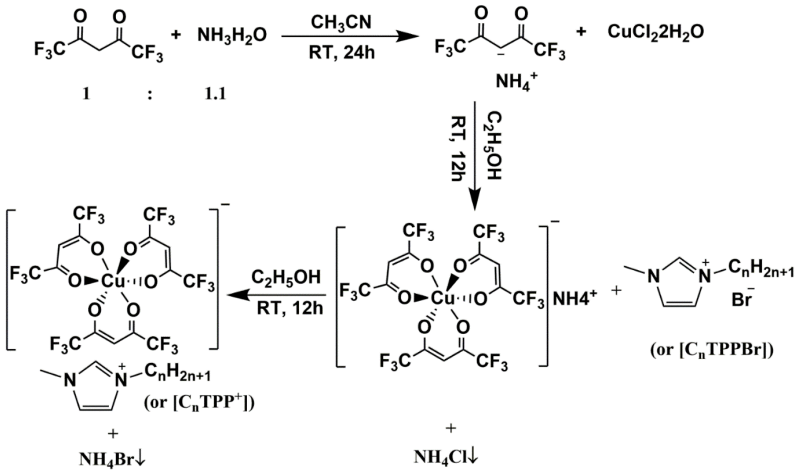

Scheme S2. Two-step approach for synthesis of ILs

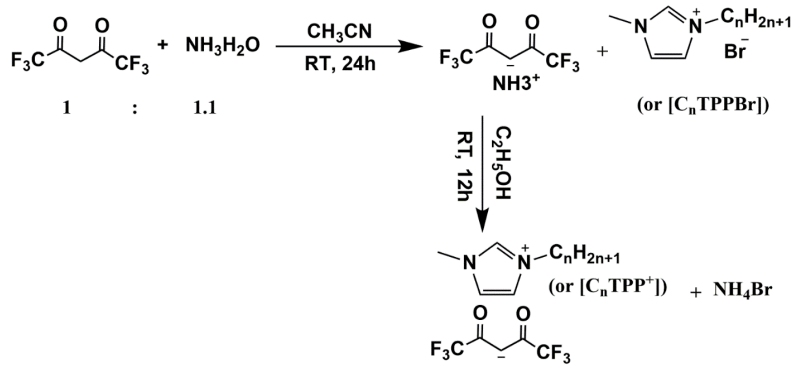

Characterization of ILs structures

The copper contents of ChILs were measured with an inductively coupled plasma spectrometer (SPECTRO ARCOS EOP), and the data obtained were as follows:

Table S1. The copper contents of ChILs measured by atomic emission spectrometry

ChILs	Cal. (%)	Exp. (%)
$[C_8mim][Cu(F_6\text{-}acac)_3]$	7.22	7.06
$[C_{10}mim][Cu(F_6\text{-}acac)_3]$	7.00	6.90
$[C_{14}TPP][Cu(F_6\text{-}acac)_3]$	5.55	5.31
$[C_{16}TPP][Cu(F_6\text{-}acac)_3]$	5.42	5.49

The contents of C, H, N of ILs were measured with an elemental analyzer (Elementar Vario EL III), and the data obtained were as follows:

Table S2. The C, H, N contents of ILs measured by elemental analysis

ILs	C		H		N	
	Cal. (%)	Exp. (%)	Cal. (%)	Exp. (%)	Cal. (%)	Exp. (%)
$[C_8mim][F_6\text{-}acac]$	50.74	50.35	6.01	5.82	6.96	7.07
$[C_{10}mim][F_6\text{-}acac]$	53.02	52.49	6.56	6.65	6.51	6.84
$[C_{14}TPP][F_6\text{-}acac]$	66.65	66.30	6.80	6.46	0.00	<0.05
$[C_{16}TPP][F_6\text{-}acac]$	67.42	67.08	7.11	7.17	0.00	<0.05

ESI-MS and ^1H NMR information:

$[C_8mim][F_6\text{-}acac]$: ESI-MS: $[C_8mim]^+$ 195.18489; $[F_6\text{-}acac]^-$ 206.98737. ^1H NMR: δH (600 MHz; DMSO-d6) 0.82 (3 H, t), 1.23 (10 H, m), 1.75 (2 H, m), 3.86 (3 H, s), 4.15 (2 H, t), 5.32 (1 H, s), 7.70 (1 H, t), 7.79 (1 H, t), 9.35 (1 H, s).

$[C_{10}mim][F_6\text{-}acac]$: ESI-MS: $[C_{10}mim]^+$ 223.21621; $[F_6\text{-}acac]^-$ 206.98741. ^1H NMR: δH (600 MHz; DMSO-d6) 0.83 (3 H, t), 1.23 (14 H, m), 1.75 (2 H, m), 3.85 (3 H, s), 4.14 (2 H, t), 5.29 (1 H, s), 7.70 (1 H, t), 7.77 (1 H, t), 9.29 (1 H, s).

$[C_{14}TPP][F_6\text{-}acac]$: ESI-MS: $[C_{14}TPP]^+$ 459.31579; $[F_6\text{-}acac]^-$ 206.98751. ^1H NMR: δH (600 MHz; DMSO-d6) 0.82 (3 H, t), 1.23 (20 H, m), 1.45 (2 H, m), 1.53 (2 H, m), 3.59 (2 H, m), 5.30 (1 H, s), 7.75–7.87 (15 H, m).

$[C_{16}TPP][F_6\text{-}acac]$: ESI-MS: $[C_{16}TPP]^+$ 487.34774; $[F_6\text{-}acac]^-$ 206.98754. ^1H NMR: δH (600 MHz; DMSO-d6) 0.82 (3 H, t), 1.21 (24 H, m), 1.43 (2 H, m), 1.51 (2 H, m), 3.55 (2 H, m), 5.25 (1 H, s), 7.75–7.87 (15 H, m).

Since the copper in ChILs is paramagnetic, it tends to form a single peak:

$[C_8mim][Cu(F_6\text{-}acac)_3]$: ESI-MS: $[C_8mim]^+$ 195.18487; $[Cu(F_6\text{-}acac)_3]^-$ 683.89269. ^1H NMR: δH (600 MHz; DMSO-d6) 0.77 (3 H, t), 1.16 (10 H, s), 1.69 (2 H, s), 3.78 (3 H, s), 4.07 (2 H, t), 7.70 (1 H, s), 7.62 (1 H, s), 9.12 (1 H, s).

$[C_{10}mim][Cu(F_6\text{-}acac)_3]$: ESI-MS: $[C_{10}mim]^+$ 223.21597; $[Cu(F_6\text{-}acac)_3]^-$ 683.89270. ^1H NMR: δH (600 MHz; DMSO-d6) 0.79 (3 H, t), 1.17 (14 H, s), 1.70 (2 H, s), 3.79 (3 H, s), 4.09 (2 H, t), 7.64 (1 H, s), 7.71 (1 H, s), 9.13 (1 H, s).

$[C_{14}TPP][Cu(F_6\text{-}acac)_3]$: ESI-MS: $[C_{14}TPP]^+$ 459.31602; $[Cu(F_6\text{-}acac)_3]^-$ 683.89340. ^1H NMR: δH (600 MHz; DMSO-d6) 0.81 (3 H, t), 1.19 (20 H, m), 1.40 (2 H, m), 1.47 (2 H, m), 3.50 (2 H, m), 7.73–7.85 (15 H, m).

$[C_{16}TPP][Cu(F_6\text{-}acac)_3]$: ESI-MS: $[C_{16}TPP]^+$ 487.34736; $[Cu(F_6\text{-}acac)_3]^-$ 683.89297. ^1H NMR: δH (600 MHz; DMSO-d6) 0.80 (3 H, t), 1.17 (24 H, m), 1.39 (2 H, m), 1.47 (2 H, m), 3.52 (2 H, m), 7.72–7.85 (15 H, m).

Determination of vaporization enthalpies of ILs by TGA

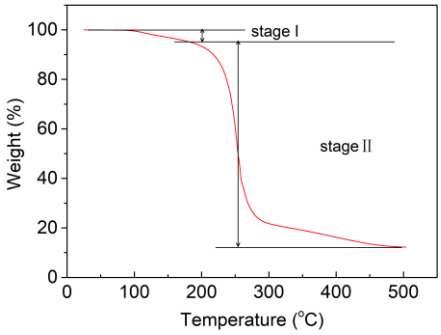

Figure S1. The ramped temperature TGA curve of [C_{10}mim][Cu(F_6-acac)$_3$] from 30 to 500 °C.

There are mainly two stages of weight loss, which are defined as stage I and stage II. Stage II is the main thermal decomposition stage of IL, while stage I might be caused by the vaporization. Then we set the experimental temperatures of the isothermal TGA method much lower the initial decomposition temperature range (around 523.2 K). For ChIL [C_{10}mim][Cu(F_6-acac)$_3$], the experimental temperatures are 413.2 K, 423.2 K, 433 K and 443.2 K.

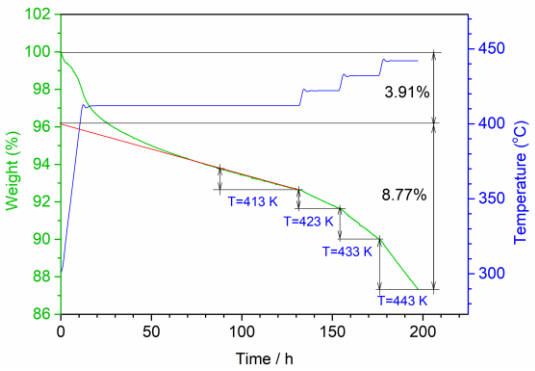

Figure S2. The typical time-course TGA weight loss measurements for ChIL [C_{10}mim][Cu(F_6-acac)$_3$] at four discrete temperatures: 413.2 K, 423.2 K, 433.2 K and 443.2 K. The green line and the blue line are with respect to time, respectively. And the red line is the tangent extension line of weightlessness curve at 413.2 K. The difference between the green and red terminate on the Y-axis is the weight loss of removal of volatile impurities. For [C_{10}mim][Cu(F_6-acac)$_3$], a temperature program was adopted: First, a heating ramp of 10 K·min^{-1} was used, followed by a 2 h static hold period at 413.2 K, allowing for the slow removal of volatile impurities. Then held at 423.2 K, 433.2 K, 443.2 K respectively for 20min. The average temperature T_{av} was 428.2 K.

According to the weight loss curve (the green line in Figure S1) in TGA process, the weight loss can be divided into two stages. The first stage was non-linear weight loss, which may be caused by volatilization of volatile impurities. The weight loss of volatile impurities was 3.91% obtained by extending the linear weight loss curve to the Y-axis (the red line). The second stage was linear weight loss (8.77%), which may be caused by the vaporization of ChIL [C_{10}mim][Cu(F_6-acac)$_3$].

Plot the sample weight vs time at four discrete temperatures (413.2 K, 423.2 K, 433 K and 443.2 K) and the weight loss rate dm / dt at each static hold period was calculated by linear correlation (Figure S3).

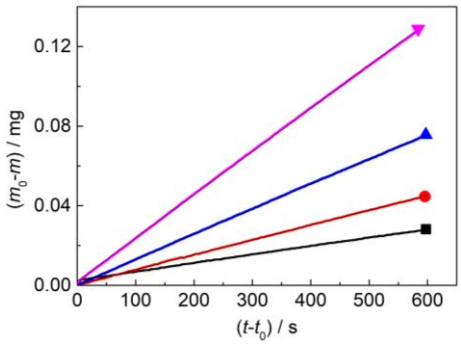

Figure S3. Plot of $(m_0 - m)$ / mg vs $(t - t_0)$ / s for $[C_{10}mim][Cu(F_6\text{-acac})_3]$. four static hold periods at 413.2 K, 423.2 K, 433.2 K and 443.2 K.-■ 413.2 K: $y = 4.28 \times 10^{-5}x + 2.56 \times 10^{-3}$, $r = 0.99953$; ●423.2 K: $y = 7.47 \times 10^{-5}x + 3.37 \times 10^{-4}$, $r = 0.99993$; ▲433.2 K: $y = 1.26 \times 10^{-4}x + 4.62 \times 10^{-4}$, $r = 0.99995$;▼443.2 K: $y = 2.17 \times 10^{-4}x + 2.09 \times 10^{-3}$, $r = 0.99995$.

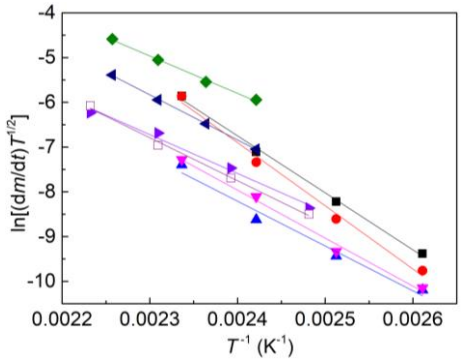

Figure S4. Plot of $\ln[(-dm/dt)\ T^{1/2}]$ vs $1/T$ for eight ILs: ■ $[C_8mim][F_6\text{-acac}]$: $y = -1.27 \times 10^4x + 23.84$, $r = -0.99862$; ● $[C_{10}mim][F_6\text{-acac}]$: $y = -1.41 \times 10^4x + 26.99$, $r = -0.99611$; ▲ $[C_{14}TPP][F_6\text{-acac}]$: $y = -1.00 \times 10^4x + 17.78$, $r = -0.98849$; ▼ $[C_{16}TPP[F_6\text{-acac}]$: $y = -1.10 \times 10^4x + 18.45$, $r = -0.99721$; ◆ $[C_8mim][Cu(F_6\text{-acac})_3]$: $y = -8.341 \times 10^3x + 14.22$, $r = -0.99821$; ◀$[C_{10}mim][Cu(F_6\text{-acac})_3]$: $y = -1.008 \times 10^4x + 17.34$, $r = -0.99983$; ▶ $[C_{14}TPP][Cu(F_6\text{-acac})_3]$: $y = -8.673 \times 10^3x + 13.23$, $r = -0.99419$; □ $[C_{16}TPP][Cu(F_6\text{-acac})_3]$: $y = -9.608 \times 10^3x + 15.31$, $r = -0.99827$; x: T^{-1}; y: $\ln[(dm/dt)T^{1/2}]$.

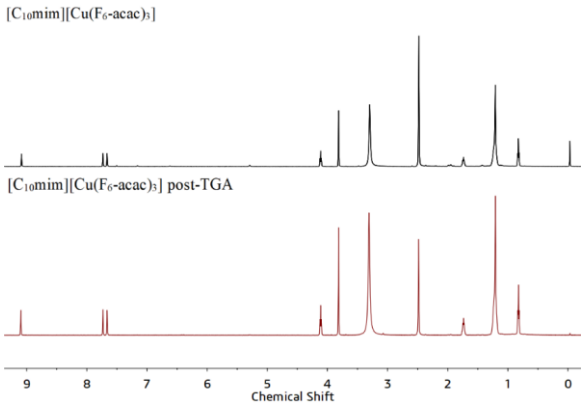

Figure S5. ^1H NMR spectra (600 MHz, DMSO) of $[C_{10}mim][Cu(F_6\text{-acac})_3]$ before (upper) and after (lower) the isothermal TGA in the main text

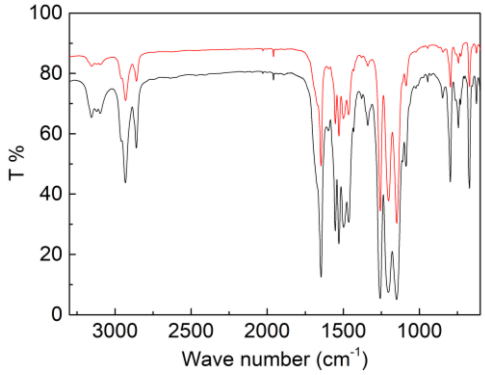

Figure S6. FTIR spectra of $[C_{10}mim][Cu(F_6\text{-}acac)_3]$ before (the black line) and after (the red line) the isothermal TGA in the main text

Table S3. The copper contents of ChIL $[C_{10}mim][Cu(F_6\text{-}acac)_3]$ before and after TGA measured by atomic emission spectrometry

Sample	Temperature (K)	Time (h)	Weight loss (%)	Copper content (%)
Initial sample [a]	/	/	/	6.90
Post-TGA	413.2–443.2	3	12.7	7.00
1	413.2	5	11.2	6.98
2	423.2	4	13.8	6.95
3	433.2	2.5	14.4	6.89
4	443.2	2	20.7	6.93
5	473.2	1	32.0	6.94

[a] The calculated copper content of $[C_{10}mim][Cu(F_6\text{-}acac)_3]$ is 7.00%.

If all the weight loss of $[C_{10}mim][Cu(F_6\text{-}acac)_3]$ in the isothermal TGA process came from vaporization, the copper content after TGA should be close to the calculated value. As shown in Table S3, the copper content of $[C_{10}mim][Cu(F_6\text{-}acac)_3]$ before TGA was 6.90%, which was lower than the calculated value (7.00%) because of the existence of volatile impurities. The copper content after TGA was 7.00%, which was consistent with the calculated value. To further verify that all the weight loss of ChILs came from vaporization during the TGA process, we kept ChIL $[C_{10}mim][Cu(F_6\text{-}acac)_3]$ at 413.2, 423.2, 433.2, 443.2, 473.2 K for 5, 4, 2.5, 2, 1 hours, respectively, to ensure that there was an evident weight loss. The copper contents of the residual samples in the crucible were measured, and the value were also close to the calculated value (7.00%), indicating that ChIL did not decompose at 413.2–473.2 K.

Physicochemical properties of ILs

Mettler Toledo DL32 Karl Fischer Coulometer was used to measure the containing of water in ILs. And the water contents of eight ILs [C_nTPP][Cu(F_6-acac)$_3$] (n = 14, 16), [$C_n$mim][Cu(F_6-acac)$_3$] (n = 8, 10), [C_nTPP][F_6-acac] (n = 14, 16) and [$C_n$mim][F_6-acac] (n = 8, 10) were lower than 500ppm.

All chromatographic analyses were performed at room temperature using a Thermo Scientific Dionex ICS-5000+ ion chromatography analyzer. The eluent was 15 mM KOH and an anion suppressor was used. The pump flow rate is 1 mL / min. The injection volume was 25 µL.

Due to the low solubility of our ILs in water, IC samples were prepared by dissolving 0.03-0.08 g ILs in 2.5-3.5 mL acetonitrile before being diluted to 10 mL with deionized water.

Table S4. The bromide contents of ILs measured by ion chromatography

IL	Br content (ppm)
[C_8mim][F_6-acac]	90.7
[C_{10}mim][F_6-acac]	104
[C_{14}TPP][F_6-acac]	169
[C_{16}TPP][F_6-acac]	172
[C_8mim][Cu(F_6-acac)$_3$]	139
[C_{10}mim][Cu(F_6-acac)$_3$]	144
[C_{14}TPP][Cu(F_6-acac)$_3$]	132
[C_{16}TPP][Cu(F_6-acac)$_3$]	90.2

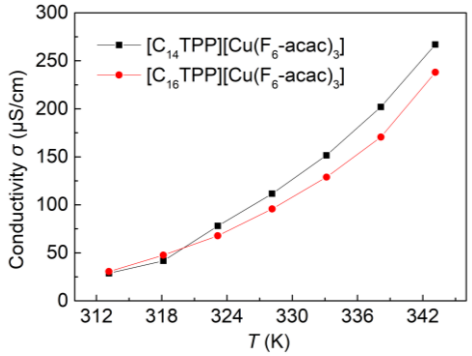

Figure S7. Plot of conductivity σ vs T of [C_nTPP][Cu(F_6-acac)$_3$] (n = 14, 16)

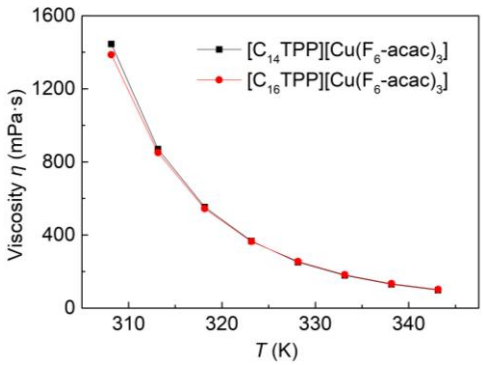

Figure S8. Plot of viscosity η vs T of [C_nTPP][Cu(F_6-acac)$_3$] (n = 14, 16)

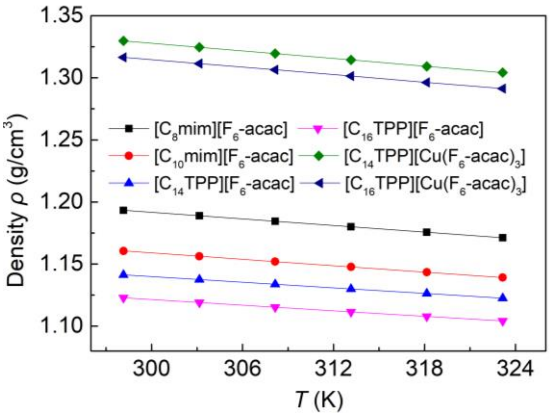

Figure S9. Plot of density ρ vs T of ILs

The relationship between density and temperature satisfies the following empirical equation: $\ln [\rho\ (\mathrm{g \cdot cm^{-3}})] = c - \alpha(T\ (\mathrm{K}) - 298)$. Where ρ is the density, c is an empirical constant, α is the thermal expansion coefficient ($\alpha = -(\partial \ln \rho / \partial T)_p$).

Table S5. The coefficient of thermal expansion, α, of ILs

IL	$10^4\ \alpha$
$[C_8mim][F_6\text{-acac}]$	8.808
$[C_{10}mim][F_6\text{-acac}]$	8.570
$[C_{14}TPP][F_6\text{-acac}]$	7.487
$[C_{16}TPP][F_6\text{-acac}]$	7.432
$[C_{14}TPP][Cu(F_6\text{-acac})_3]$	7.741
$[C_{16}TPP][Cu(F_6\text{-acac})_3]$	7.737

Mass spectrometry data

The **LCMS** (ESI) for [C_8mim][F_6-acac]. *m/z* for [C_8mim]$^+$ 195.18489, for [F_6-acac]$^-$ 206.98737.

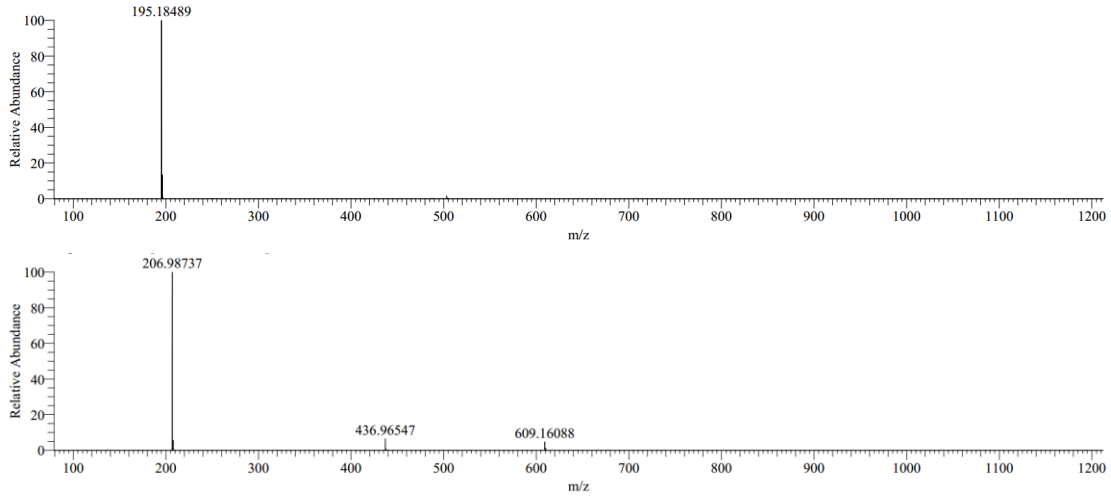

The **LCMS** (ESI) for [C_{10}mim][F_6-acac]. *m/z* for [C_{10}mim]$^+$ 223.21621, for [F_6-acac]$^-$ 206.98741.

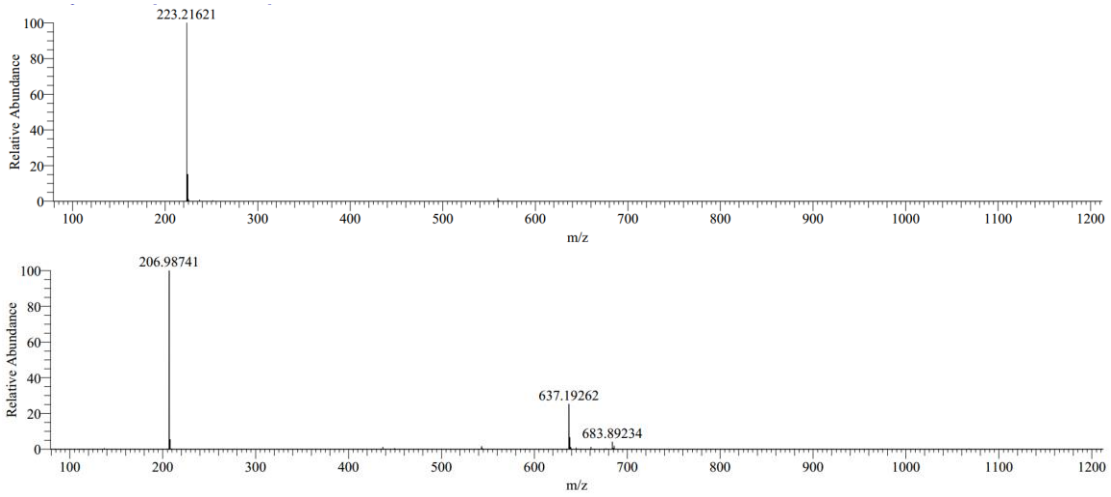

The **LCMS** (ESI) for $[C_{14}TPP][F_6\text{-acac}]$. *m/z* for $[C_{14}TPP]^+$ 459.31579, for $[F_6\text{-acac}]^-$ 206.98751.

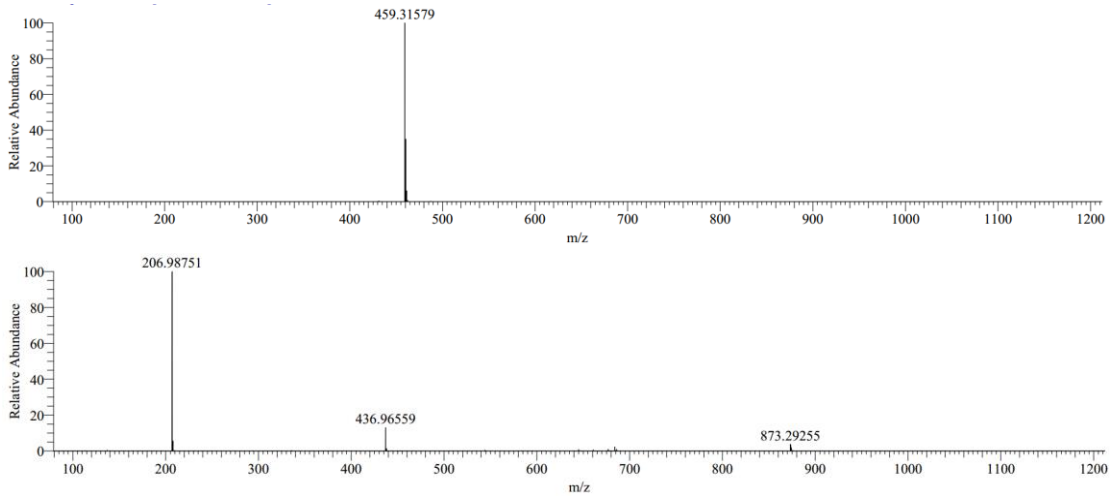

The **LCMS** (ESI) for $[C_{16}TPP][F_6\text{-acac}]$. *m/z* for $[C_{16}TPP]^+$ 487.34774, for $[F_6\text{-acac}]^-$ 206.98754.

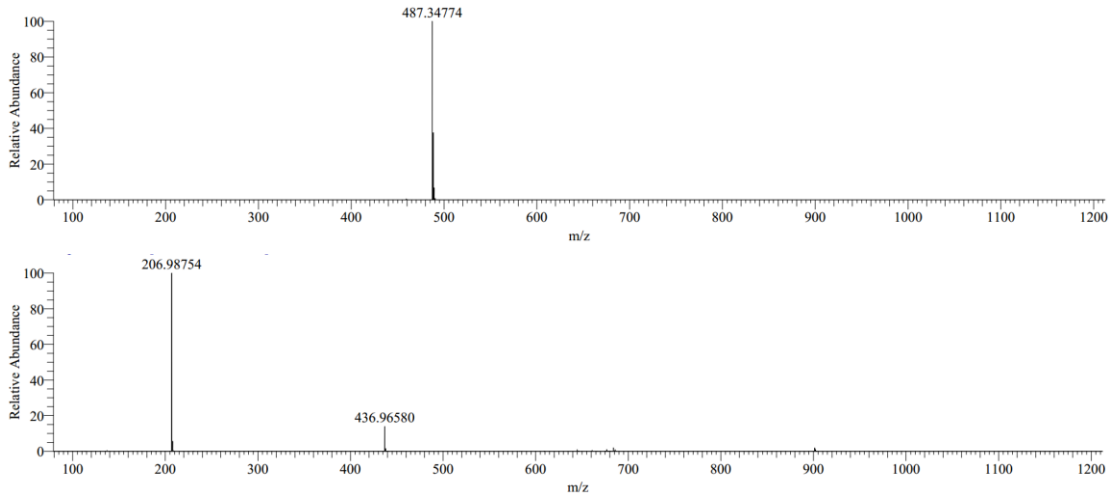

The **LCMS** (ESI) for $[C_8mim][Cu(F_6\text{-}acac)_3]$. *m/z* for $[C_8mim]^+$ 195.18487, for $[Cu(F_6\text{-}acac)_3]^-$ 683.89269.

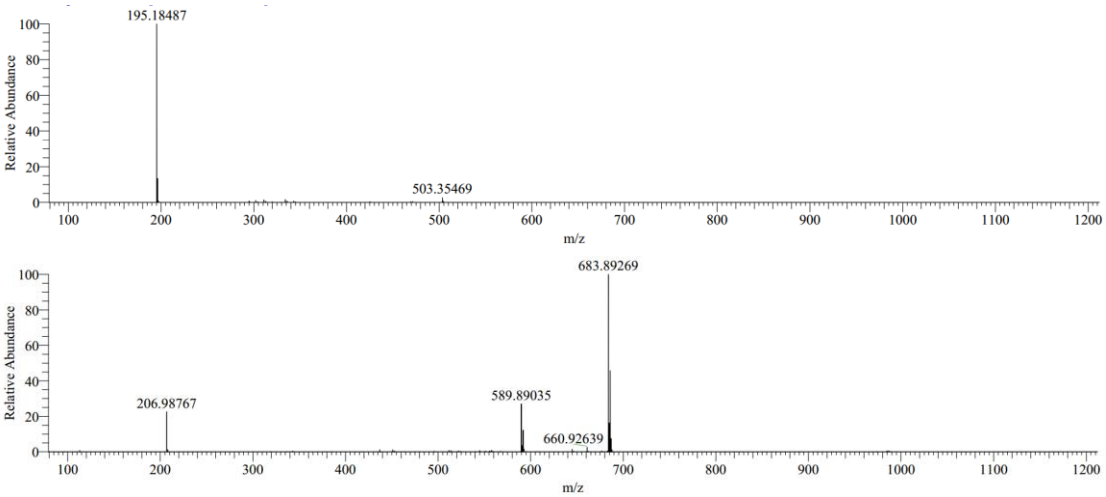

The **LCMS** (ESI) for $[C_{10}mim][Cu(F_6\text{-}acac)_3]$. *m/z* for $[C_{10}mim]^+$ 223.21597, for $[Cu(F_6\text{-}acac)_3]^-$ 683.89270.

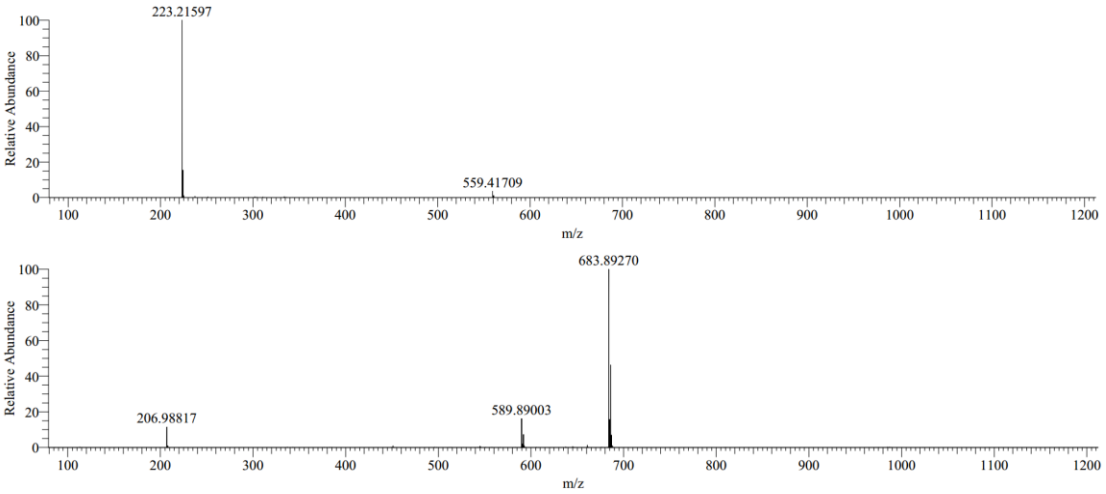

The **LCMS** (ESI) for $[C_{14}TPP][Cu(F_6\text{-acac})_3]$. *m/z* for $[C_{14}TPP]^+$ 459.31602, for $[Cu(F_6\text{-acac})_3]^-$ 683.89340.

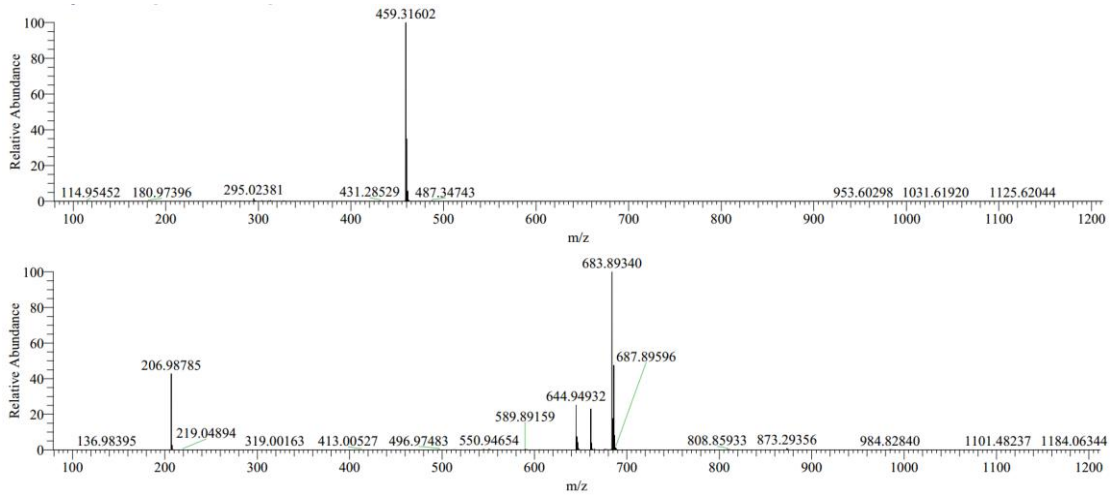

The **LCMS** (ESI) for $[C_{16}TPP][Cu(F_6\text{-acac})_3]$. *m/z* for $[C_{16}TPP]^+$ 487.34736, for $[Cu(F_6\text{-acac})_3]^-$ 683.89297.

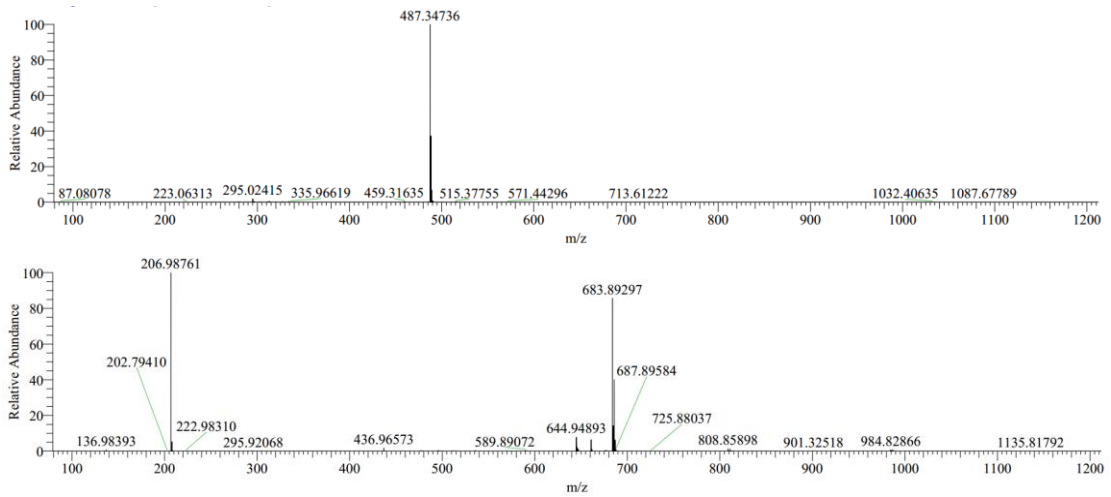

^{1}H NMR spectroscopic data

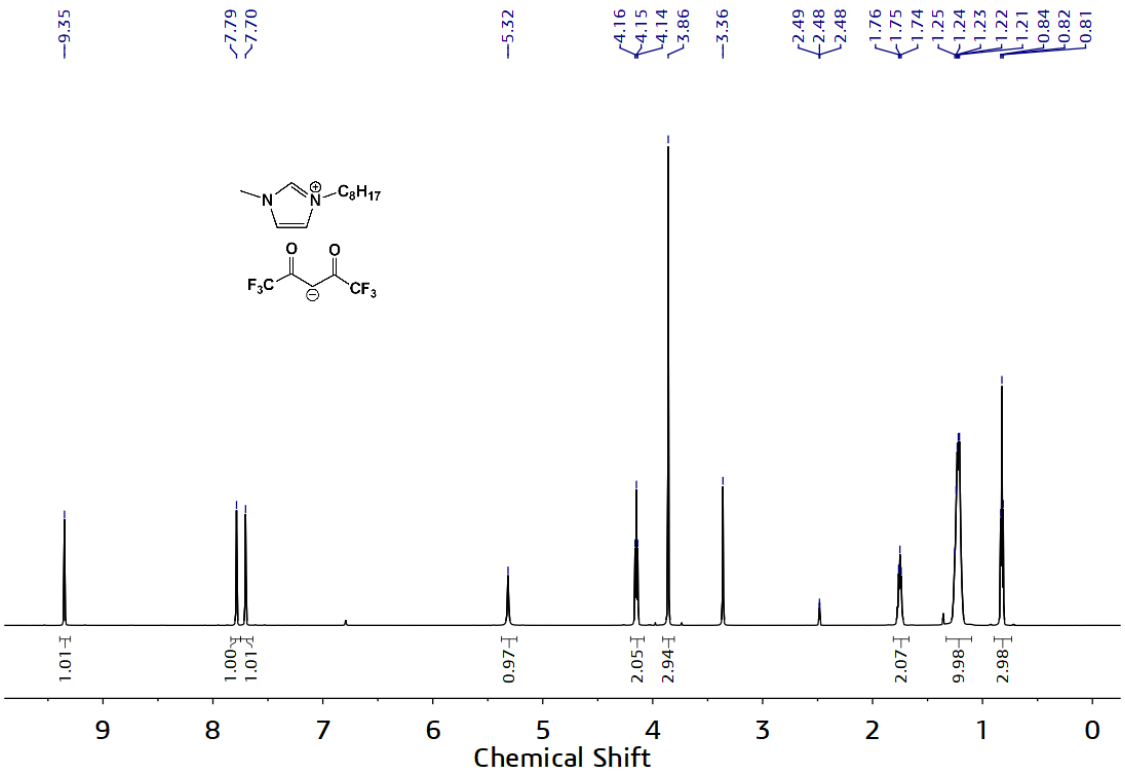

^{1}H NMR (600 MHz, DMSO-d6) of [C_8mim][F_6-acac].

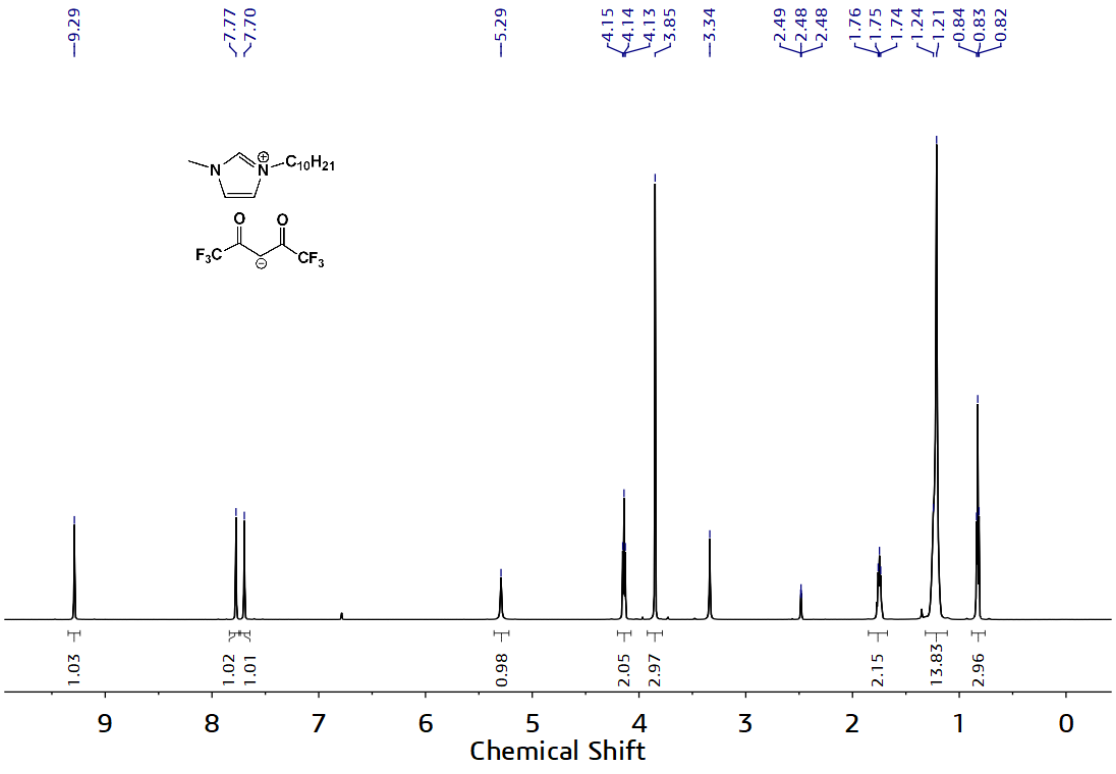

^{1}H NMR (600 MHz, DMSO-d6) of [C_{10}mim][F_6-acac].

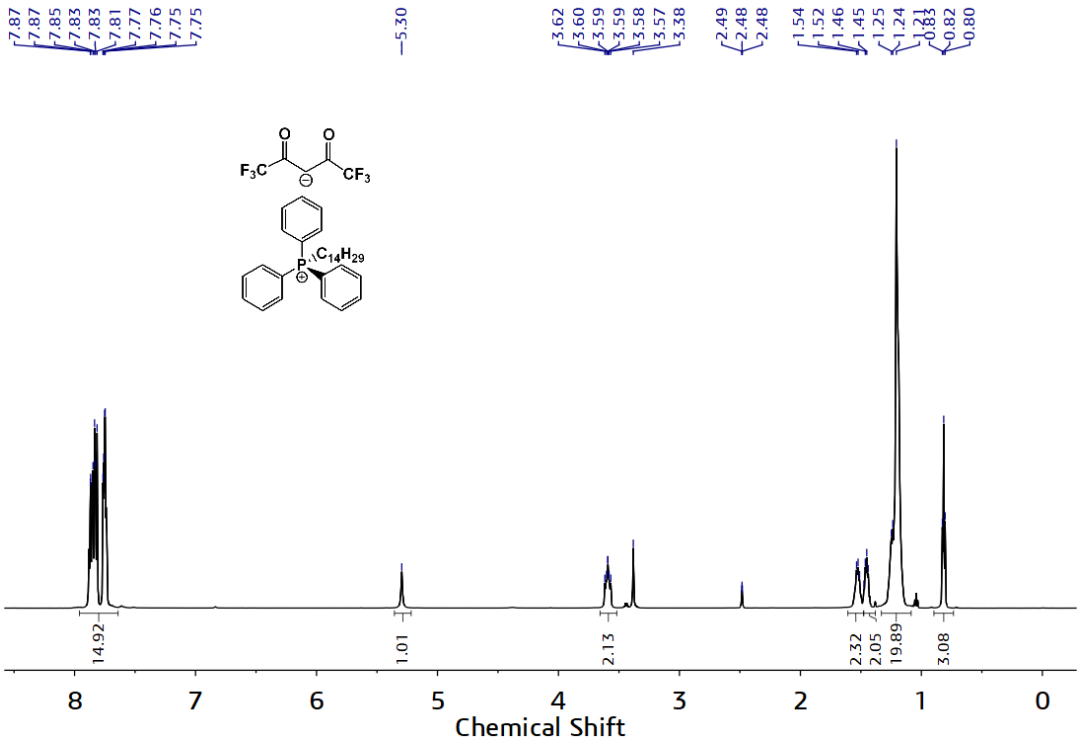

^{1}H NMR (600 MHz, DMSO-d6) of [C_{14}TPP][F_6-acac].

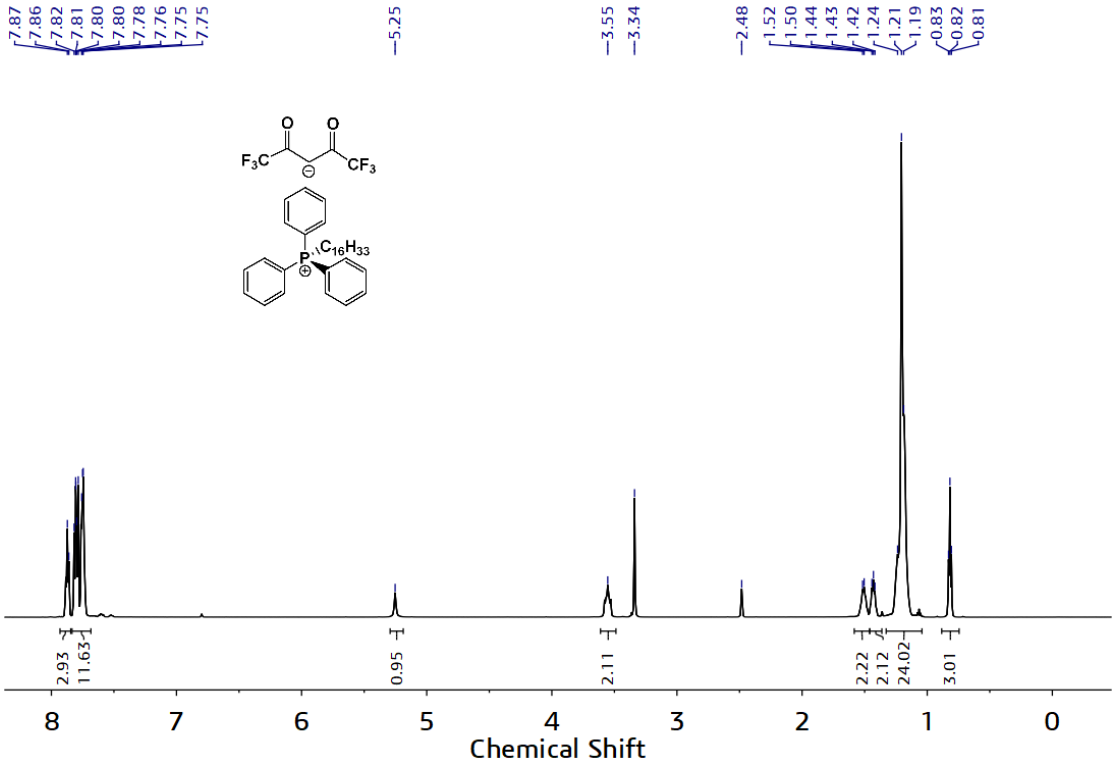

^{1}H NMR (600 MHz, DMSO-d6) of [C_{16}TPP][F_6-acac].

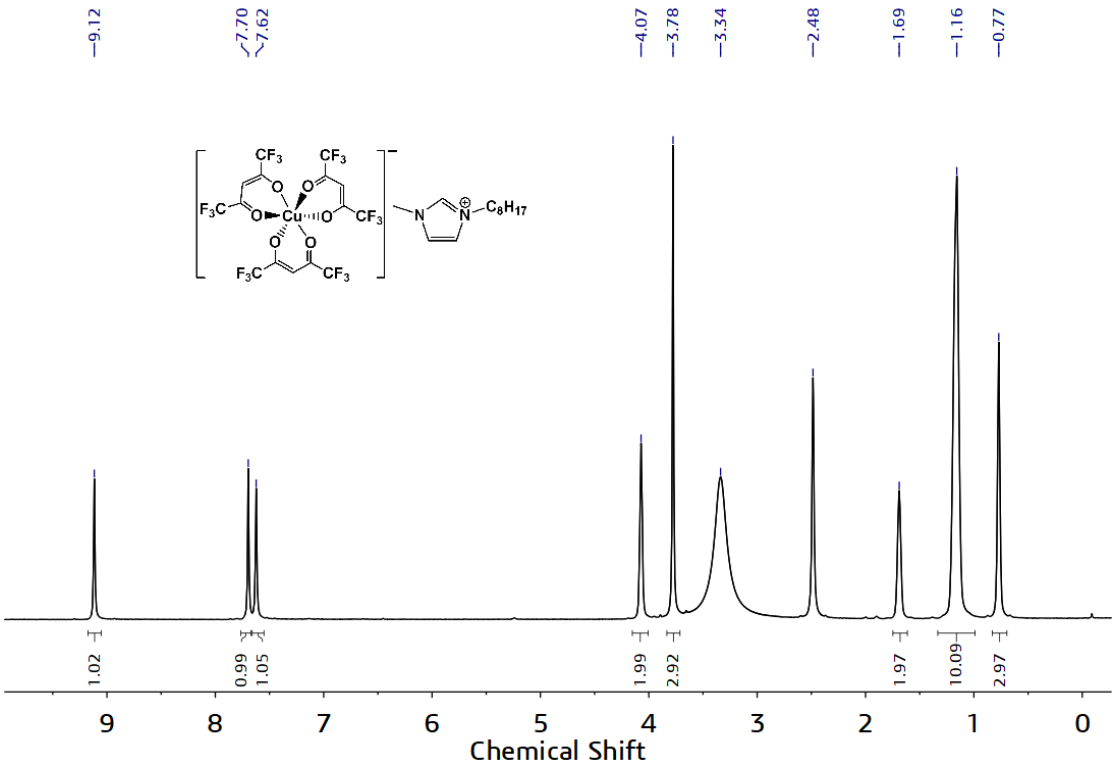

^{1}H NMR (600 MHz, DMSO-d6) of [C_8mim][Cu(F_6-acac)$_3$].

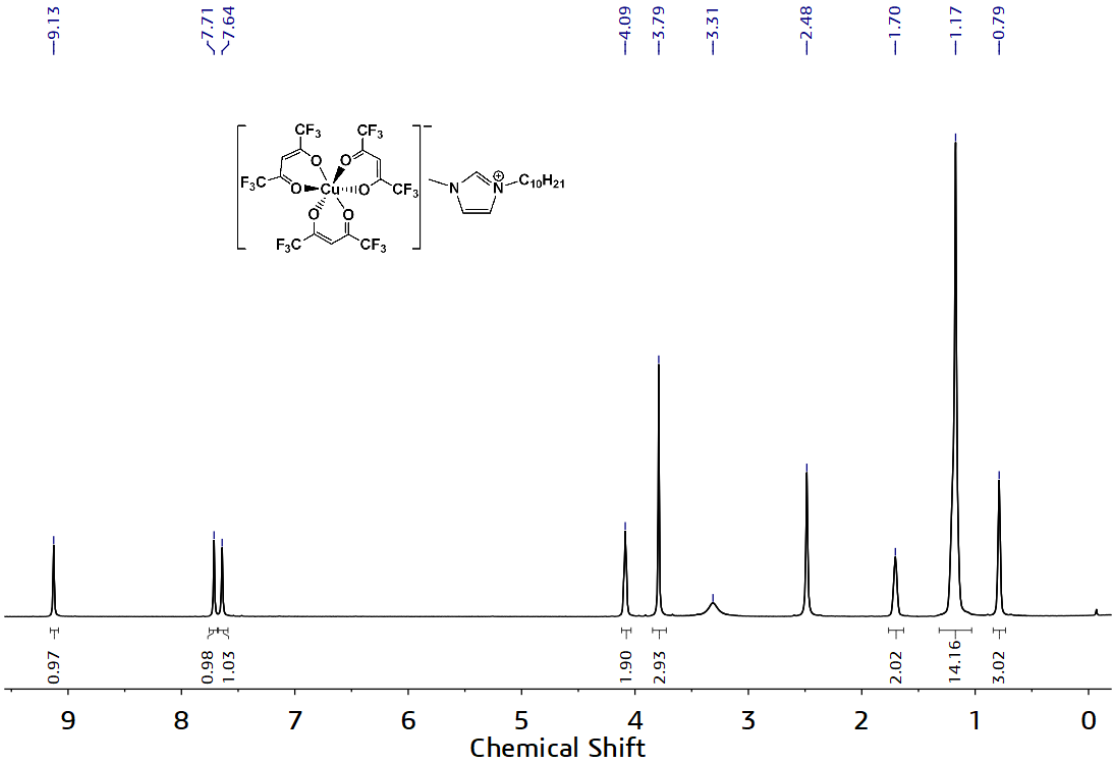

^{1}H NMR (600 MHz, DMSO-d6) of [C_{10}mim][Cu(F_6-acac)$_3$].

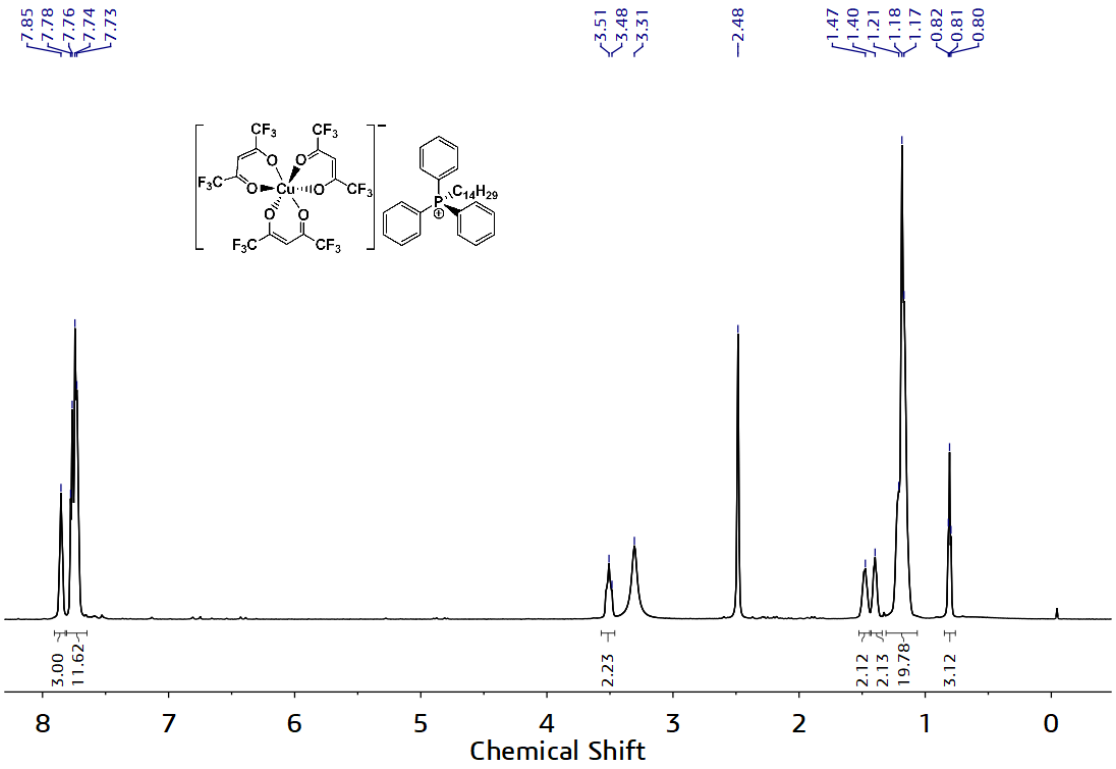

^{1}H NMR (600 MHz, DMSO-d6) of $[C_{14}TPP][Cu(F_6\text{-acac})_3]$.

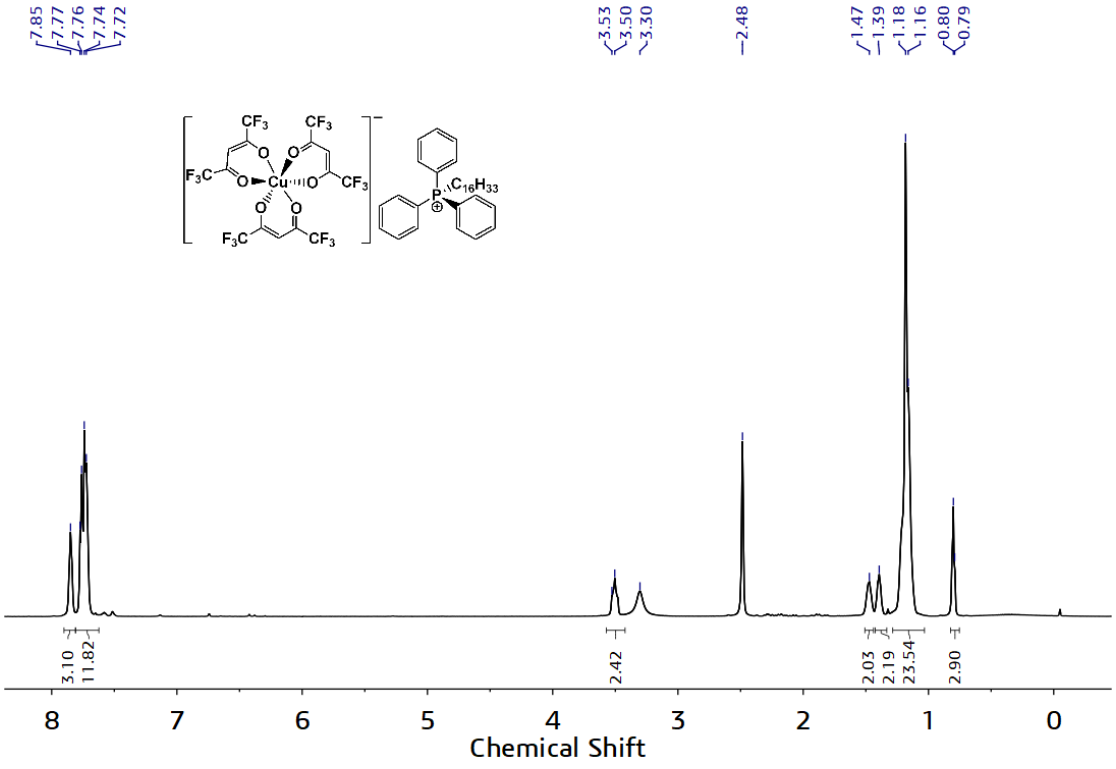

^{1}H NMR (600 MHz, DMSO-d6) of $[C_{16}TPP][Cu(F_6\text{-acac})_3]$.